ACS OMEGA

Open Access

http://pubs.acs.org/journal/acsodf

Article

Preparation of a Water-Soluble Glycopolymer Bearing Porphyrin Skeletons and Its Biological Properties

Yoshihiro Ishimaru, Tomohide Moteki, Miho Suzuki, Tetsuo Koyama, Takahiko Matsushita, Ken Hatano, and Koji Matsuoka*

Cite This: *ACS Omega* 2023, 8, 37451−37460

Read Online

ACCESS | Metrics & More | Article Recommendations | Supporting Information

ABSTRACT: A known tetraphenyl porphyrin (TPP) having an amino functional group [5-(4-aminophenyl)-10,15,20-(triphenyl)-porphyrin] was converted into the corresponding monomer by means of condensation with acryloyl chloride. Simple radical polymerization of the porphyrin monomer and a glycosyl monomer in the presence of acrylamide as a regulator monomer in order to avoid steric interference gave a water-soluble glycopolymer bearing porphyrin moieties. Spectroscopic analyses suggested incorporation of porphyrin moieties in the glycopolymer. The physical properties of the water-soluble glycopolymer bearing porphyrin moieties were examined in aqueous media, and the results also indicated the incorporation of TPP moieties in the polymer. Uptake of the polymer into HeLa cells was observed, and the cytotoxicity of the polymer was confirmed by microscopic analyses. The glycopolymer bearing porphyrin moieties is promising not only for photodynamic therapy but also as an anti-cancer reagent.

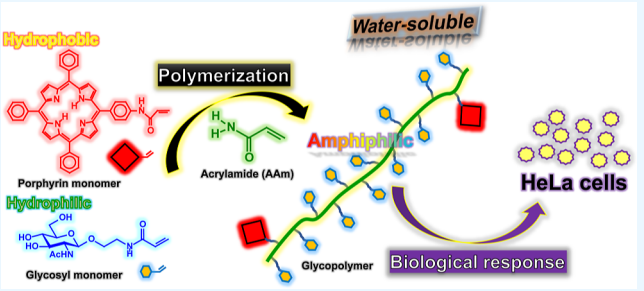

INTRODUCTION

A typical porphyrin family member is a macrocyclic derivative having four pyrrole residues connected with four methine bridges, and a porphine ring system is a 16-member ring system with 22 π electrons, in which 18 π electrons show an 18 π-electron conjugated system giving their tautomer.[1] In addition, the porphyrin derivatives show aromaticity because the 18 π-electron conjugated system of the porphyrin ring system fulfills the Hückel rule,[2,3] and the porphyrin skeleton forms a planar structure.[4] According to the π electronic transition on the 26 π electrons in porphyrin derivatives, the porphyrin derivatives strongly absorb as the Soret band at around 400 nm due to $\pi-\pi^*$ transition and as the Q band at around 480−650 nm due to vibration of their own molecular structure.

Although normal tissues do not retain porphyrins, tumors accumulate porphyrin.[5−7] The Soret band and the Q band are excited by a laser beam of around 630 nm giving the corresponding energy for activation of oxygen to afford a highly active oxygen species, so-called singlet oxygen,[8] which attacks ambient cancer cells to yield the extinction of the cells. Photodynamic diagnosis (PDD)[9,10] and photodynamic therapy (PDT)[11−13] by means of porphyrin derivatives are used in medical approaches for detection and treatment of cancers. Since protoporphyrins accumulate in cancer tissues, PDD can reveal the cancer tissues by means of red illumination caused by laser excitation around 630 nm.[14] PDD can be used to detect a superficial cancers, such as skin cancer, lung cancer, and colorectal cancer.[15] On the other hand, in PDT, a photosensitizer is activated by an appropriate laser light to induce a photochemical reaction in a malignant tumor that causes significant damage to the tumor tissues.[8] PDT has the benefit of low strain compared to a surgical operation and shows an attractive characteristic by contribution to improvement of quality of life for a patient.[16] In addition, treatment of early-stage lung cancer, esophageal cancer, stomach cancer, and an early-stage cervical lesion by means of endoscopic PDT is human-friendly and efficient and shows a large number of merits. However, after injection of a synthetic photosensitizer, slow excretion and accumulation of the photosensitizers in the body are problems. Since the solubility of synthetic photosensitizers in aqueous media is low, it is thought that the metabolism of photosensitizers is poor. In order to resolve the problem of low solubility in aqueous media, we decided to combine a porphyrin and a carbohydrate by using polymer chemistry. Water-soluble porphyrins[17−19] and glycoporphyrins[20−22] were obtained as the hydrophilic substances in previous studies, and their applications for PDT were also examined. In this paper, we describe the preparation of two

Received: July 31, 2023
Accepted: August 29, 2023
Published: September 26, 2023

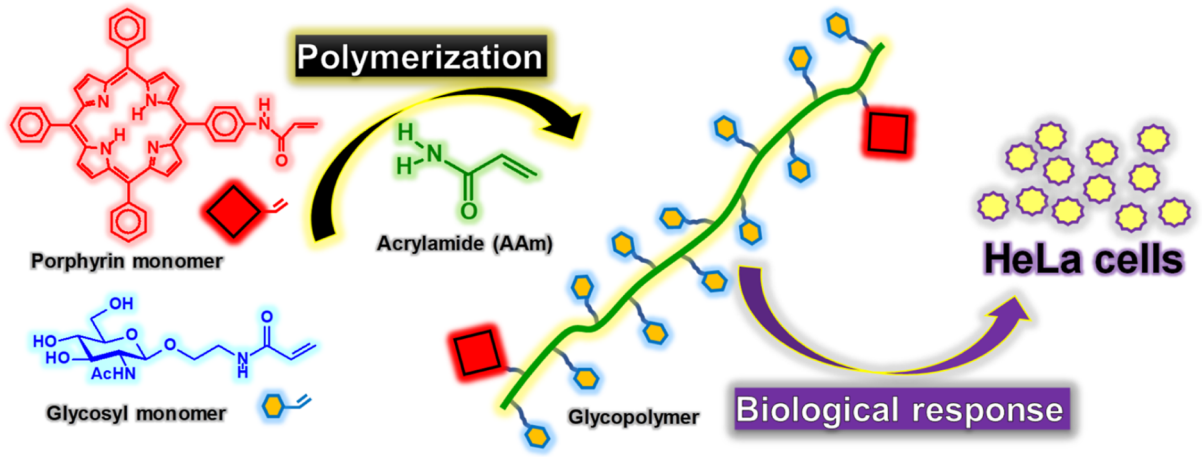

Figure 1. Water-soluble glycopolymer having porphyrin moieties was prepared from the corresponding monomers by simple radical polymerization, and the biological responses of the glycopolymer against HeLa cells were evaluated.

kinds of monomers having a porphyrin skeleton and *N*-acetyl-D-glucosamine (GlcNAc) as a model carbohydrate moiety,[23] synthetic assembly of both monomers with acrylamide (**AAm**) as a regulator for adjusting densities of each monomer unit by radical polymerization, and biological responses of the polymers for cancer cells. A schematic image of this study is shown in Figure 1, where the water-soluble glycopolymer having porphyrin moieties might show biological activities against HeLa cells.

EXPERIMENTAL SECTION

Materials and Methods. Without further purification, all commercially available solvents and reagents were used unless otherwise stated. Methanol (MeOH) was dried over 3 Å MS, and 1,2-dichloromethane (DCE) was dried over 4 Å MS before use. Acrylamide was purified by recrystallization from $CHCl_3$ and stored in a refrigerator. A known [5-(4-aminophenyl)-10,15,20-(triphenyl)porphyrin] **1**[24] was prepared from *meso*-tetraphenylporphyrin[25] by nitration[24] followed by Bechamp reduction.[26] A known acrylamido-ethyl 2-acetamido-3,4,6-tri-*O*-acetyl-D-glucopyranoside **4**[27] was prepared from 2-acetamido-1,3,4,6-tetra-*O*-acetyl-D-glucosamine by the method previously reported. IR spectra were measured using a Shimadzu IR Prestige-21 spectrometer (Shimadzu Corporation, Kyoto, Japan). NMR spectra were obtained at 400 MHz for ^{1}H and at 101 MHz for ^{13}C with a Bruker DPX-400 spectrometer (Bruker BioSpin MRI GmbH, Ettlingen, Germany) or at 500 MHz for ^{1}H and at 126 MHz for ^{13}C with a Bruker AVANCE 500 spectrometer (Bruker BioSpin MRI GmbH, Ettlingen, Germany) in chloroform-*d* ($CDCl_3$), dimethyl sulfoxide-d_6 (DMSO-d_6), or deuterium oxide (D_2O). Chemical shifts are expressed as parts per million (ppm, δ) and are relative to an internal tetramethylsilane in $CDCl_3$ (δ 0.0), CH_3 in DMSO-d_6 (δ 2.50), or HDO in D_2O (δ 4.78) for ^{1}H and $CHCl_3$ in $CDCl_3$ (δ 77.16) or CH_3 in DMSO-d_6 (δ 39.51) for ^{13}C. Ring-proton assignments in the ^{1}H NMR spectra were made by first-order analysis of the spectra and are supported by the results of homonuclear decoupling experiments and H−H or heteronuclear multiple quantum correlation experiments. Matrix-assisted laser desorption/ionization time-of-flight mass spectra were obtained using a Bruker AutoflexIII spectrometer (Bruker Daltonics, Bremen, Germany). Elemental analyses were performed with a Fisons EA1108 (Thermo Fisher Scientific Inc., Waltham, MA, USA) on samples that were extensively dried at 50−60 °C over phosphorus pentoxide for 4−5 h. Thin-layer chromatography (TLC) on a precoated plate of Silica Gel 60F_{254} (layer thickness, 0.25 mm; E. Merck, Darmstadt, Germany) was used for monitoring the reactions. To detect the intermediates, TLC plates were dipped in (a) a solution of 85:10:5 (v/v/v) MeOH−*p*-anisaldehyde−concd H_2SO_4 and heated for a few minutes (for carbohydrate) or (b) an aq solution of 5 wt % $KMnO_4$ and heated similarly (for detection of C=C double bonds). Chromatographic purifications were carried out using typical glass columns packed with silica gel (Silica Gel 60; 63−200 μm, E. Merck, Darmstadt, Germany). In addition, silica gel (Silica Gel 60, spherical neutral; 40−100 μm, E. Merck, Darmstadt, Germany) was used for flush column chromatography. Concentrations of all extractions were measured below 45 °C under reduced pressure. Purification by dialysis was performed against distilled water using a dialysis tubing [molecular cutoff (MWCO): 12 k−16 kDa, Dow Chemical Co., Midland, MI, USA]. UV-vis spectra were uncorrected and were recorded with a Shimadzu UV-2550 spectrophotometer (Shimadzu Corporation, Kyoto, Japan). Emission spectra were uncorrected and were recorded with a Shimadzu RF-5300PC fluorescence spectrophotometer (Shimadzu Corporation, Kyoto, Japan). Measurements of fluorescence emission spectra and excitation spectra were carried out in a Teflon-stoppered cuvette (12.5 mm in width × 45 mm height) containing 3.0 mL of a sample. The slit width of the excitation and emission was 5.0 nm, and the scan speed was high. The sensitivity was high and the interval of sampling was 1.0 nm.

5-(4-Acrylamidophenyl)-10,15,20-triphenylporphyrin (3). To a solution of freshly prepared aminoporphyrin **1**[24] (200 mg, 0.318 mmol) in the presence of triethylamine (Et_3N) (82.7 μL, 0.635 mmol) in 1,2-dichloroethane (4 mL) at 0 °C under a N_2 atmosphere was added dropwise acryloyl chloride (30.8 μL, 0.381 mmol) with stirring. The reaction mixture was allowed to react at rt for 4 h, and the results of TLC of the reaction mixture indicated complete consumption of the starting materials. The reaction mixture was diluted with water, and the whole mixture was extracted with $CHCl_3$. The organic layer was successively washed with 1 M aq H_2SO_4, satd aq $NaHCO_3$, and brine, dried over anhyd $MgSO_4$, filtered, and evaporated *in vacuo* to yield the corresponding syrup, which

https://doi.org/10.1021/acsomega.3c05581
ACS Omega 2023, 8, 37451−37460

Scheme 1. Chemical Synthetic Routes of Compound 3[a]

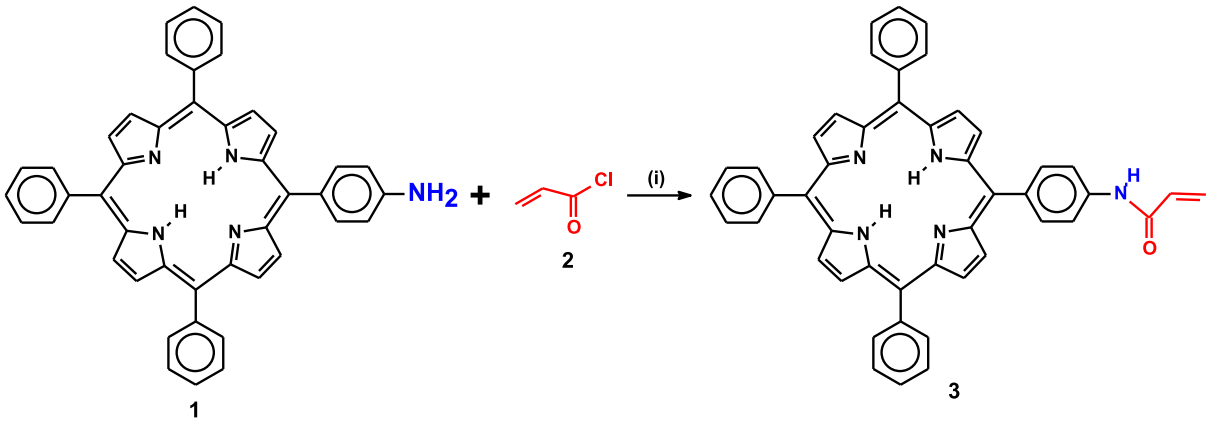

[a]Reagents and conditions: (i) triethylamine, dichloroethane, 0 °C, N_2, 4 h.

was chromatographed on silica gel with $CHCl_3$ as the eluent to afford desired **3** accompanied by side products. Further chromatographic purification was performed on silica gel with CH_2Cl_2 as the eluent to provide pure **3** (155.8 mg, 71.7%): R_f 0.5 [2:1 hexane−EtOAc (v/v)], R_f 0.23 ($CHCl_3$), R_f 0.33 (CH_2Cl_2); IR (KBr) 3316 (ν_{N-H}), 3053 (ν_{C-H}), 1670 ($\nu_{C=O}$, amide I), 1557 (δ_{N-H}, amide II) cm^{-1}; ^1H NMR δ (500 MHz, $CDCl_3$) 8.84 (s, 8H, pyrrole-β), 8.21 (m, 6H, ph-*ortho*), 8.16 (d, 2H, J_{vic} = 8.1 Hz, acrylamide-ph-*meta*), 7.91 (d, 2H, acrylamide-ph-*ortho*), 7.75 (m, 9H, ph-*meta* and -*para*), 7.51 [s, 1H, N−H (amide)], 6.56 [dd, 1H, J_{gem} = 1.3 Hz, $J_{vic\ (tras)}$ = 17.49 Hz, $=CH_2$ (*trans*)], 6.33 [dd, $J_{vic\ (cis)}$ = 10.3 Hz, =CH], 5.86 [dd, 1H, $=CH_2$ (*cis*)], −2.77 [s, 2H, N−H (pyrrole)]; MALDI-TOF MS calcd for $[M + H]^+$: 683.268. Found: *m*/*z* 683.203.

Anal. Calcd for $C_{47}H_{33}N_5O{\cdot}0.3H_2O$: C, 81.91; H, 4.91; N, 10.16. Found: C, 81.90; H, 4.93; N, 9.88.

Polymerization. A solution of a porphyrin monomer **3** (3.22 mg, 4.7 μmol), a carbohydrate monomer **4** (15 mg, 47 μmol), and acrylamide (**AAm**, 33.5 mg, 470 μmol) in DMSO was deaerated under reduced pressure for 30−60 min, and then azobis(isobutyronitrile) (AIBN, 2.32 mg, 14.1 μmol) was added under an Ar atmosphere. The mixture was stirred at 90 °C for 3 h and diluted with 0.1 M aq pyridine-acetic acid buffer (pH 5.0). The mixture was dialyzed against deionized water followed by lyophilization to give a white cotton-like polymer, which was further purified by a combination of silica gel chromatography and gel filtration with Sephadex G-50 to afford the desired glycopolymer **5** (26.4 mg).

Size Exclusion Chromatography Method. Estimation of weight-average molecular weights ($\overline{Mw}$) was done by the following conditions. Glycopolymer was analyzed by a CLASS-VP system (Shimadzu Corp., Tokyo, Japan) equipped with a Shodex Asahipak GF-510HQ column (0.46 × 250 mm, Shoko, Co., Ltd., Tokyo, Japan) at 40 °C. Prior to injection of the sample, the equilibrium of the column was accomplished with a 0.3 M NaCl aqueous solution,[28] and a flow rate of 0.300 mL/min was used for the experiment. A differential refractometer (Waters Corp., MA, USA) was used for detection of the sample. Pullulan standards (5.9, 11.8, 22.8, 47.3, 112, 212, 404, and 788 kDa; Shodex P-82) were used to obtain calibration curves.

Glycopolymer Uptake into HeLa Cells. A solution of the glycopolymer **5** (∼25 μM) in PBS (30 μL) was added to a tube containing a 3 μL dry film of BioPORTER reagent (Gene Therapy Systems, San Diego, CA, USA) and hydrated for approximately 10 min at rt. On the other hand, a solution of the glycopolymer **5** (∼25 μM) in PBS (30 μL) without BioPOTER reagent treatment was directly applied to cultured cells. Responsive solution was then suspended in 270 μL of HyClone Dulbecco's modified Eagle's medium (DMEM)/high Glucose culture medium (Thermo Fisher Scientific, Waltham, MA, USA) without fetal bovine serum (FBS) and added to HeLa cells in a 24-well culture plate under confluent conditions. The cells were incubated for 4 h at 37 °C with 5% CO_2. The removal of the residual substances was done by washing the cells with culture medium containing 10% FBS. The incubation of the cells was carried out for 1 h in the culture medium. Subsequently, the replacement of the culture medium was performed with serum-free culture medium containing apoptosis-inducing reagents.

Flow Cytometry of HeLa Cells.[29] The culture supernatant from the apoptosis-induced HeLa cells was recovered, and 250 μL of 0.2 mM EDTA was used to wash the cells. The chelating solution was removed and combined with the culture supernatant. 250 μL each of Accutase and Accumax cell detachment mixtures (Innovative Cell Technologies, San Diego, CA, USA) was used for incubation of the remaining cells for 4 h at 37 °C in the presence of glycopolymer **5** (0, 0.5, 1.0, 2.5, and 7.5 μM). The detachment mixtures with the detached cells were added to the whole recovered solution. To the culture plate was then added trypsin (0.25%, 250 μL) for complete cell detachment. The solutions containing cell debris were combined with those previously recovered, and the resulting solutions were filtered and subjected to flow cytometry analysis using a Flicyme-300 instrument (Mitsui Engineering and Shipbuilding, Tokyo, Japan). The fluorescence lifetime, fluorescence intensity, and other optical data displayed by the harvested cell population (50,000 cells) were monitored by excitation using a 440 nm semiconductor laser (60 mW). The data obtained were processed using FlowJo software (FlowJo, Ashland, OR, USA).

Microscopic Analyses of HeLa Cells in the Presence of the Glycopolymer. Just after the glycopolymer uptake into HeLa cells described above, cells were observed with a bright field of phase contrast microscopy (Nikon Eclipse TE-179 2000-U, Nikon Solutions Co. Ltd., Tokyo Japan). Briefly, HeLa cells grown in a 24-well culture plate filled with 500 μL

https://doi.org/10.1021/acsomega.3c05581
ACS Omega 2023, 8, 37451−37460

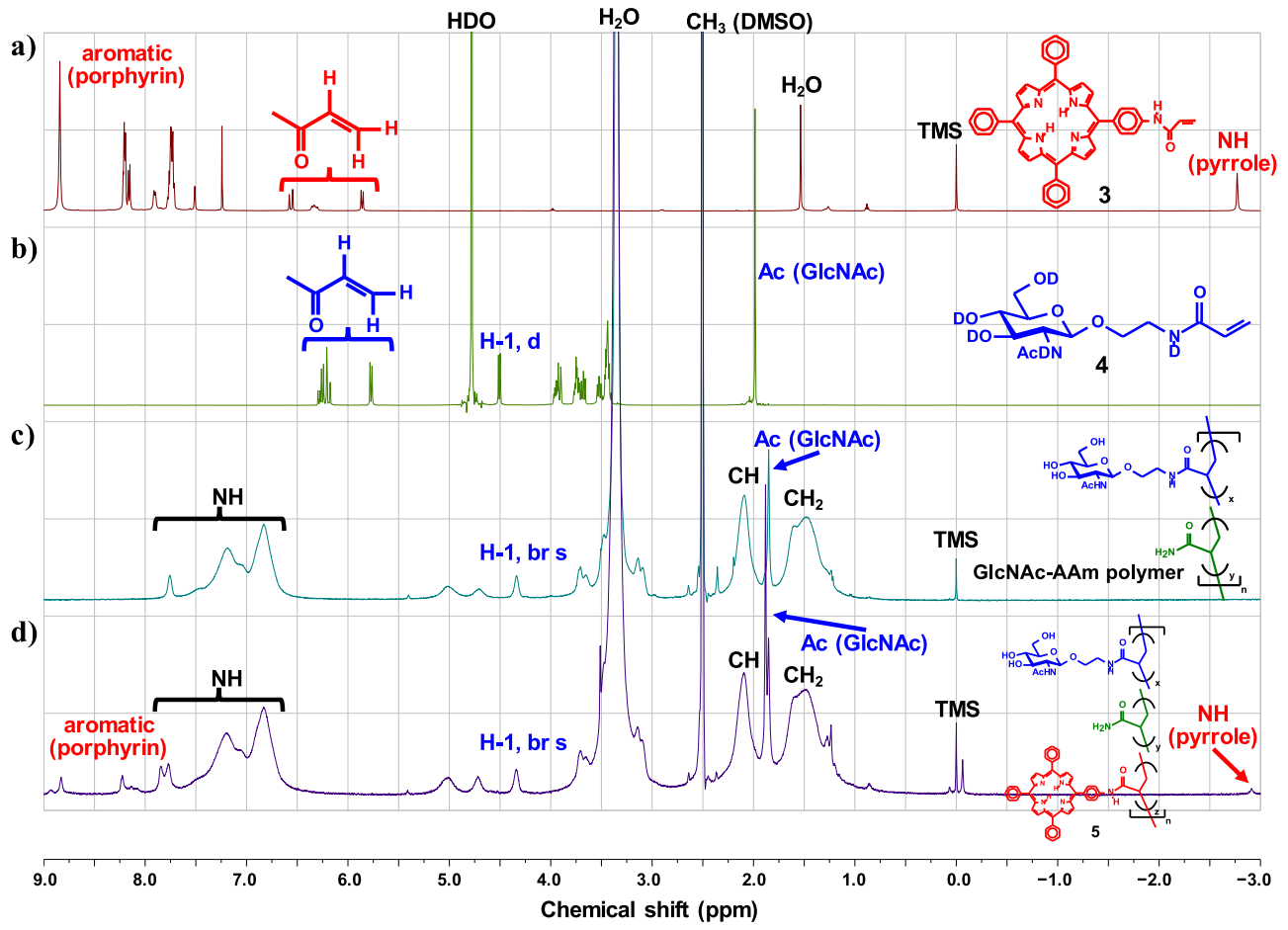

Figure 2. ^{1}H NMR spectra of TPP monomer **3** measured in DMSO-d_6 (a), GlcNAc monomer **4** measured in D_2O (b), copolymer of GlcNAc **4** with **AAm** measured in DMSO-d_6 (c), and water-soluble glycopolymer bearing porphyrin moieties **5** measured in DMSO-d_6 (d).

of DMEM supplied with 10% FBS including an appropriate concentration of the glycopolymer **5** were cultured for 4 h at 37 °C under a 5% CO_2 atmosphere. The cells were then washed with 500 μL aliquots of DMEM supplied with 10% FBS and filled with the same culture medium for observation with microscopy using 10× eyepiece and 40× objective lens.

Induction of Apoptosis in HeLa Cells. Just after glycopolymer uptake into HeLa cells following 1 h of additional incubation with the fresh culture medium described above, cells were induced apoptosis with the chemical reagent. Briefly, glycopolymer uptake HeLa cells were incubated in HyClone DMEM/high glucose culture medium supplemented with 10% FBS for 1 h. The medium was then replaced with FBS-free culture medium in the presence or absence of serum. Appropriate amounts of tumor necrosis factor alpha (TNF-α, 100 ng/mL) and low (0.5 mg/mL) or high (2 mg/mL) doses of 4-dimethyl-2-oxocyclohexyl]-2-hydroxyethyl-27-piperidine-2,6-dione (cycloheximide, CHX) were added to the fresh medium. The treated cells were incubated for 6 h before harvesting for microscopic or flow cytometric investigations.

RESULTS AND DISCUSSION

Synthesis of the Water-Soluble Glycopolymer Having TPP Moieties. Many efforts have been made for the chemical syntheses of various porphyrin derivatives, and the *meso* position in the porphyrin skeleton can be modified conveniently in order to attach other functional groups as well as molecules. We decided to use a tetraphenyl porphyrin (TPP) as a model molecule because of it being easy to handle and its convenient access. The known TPP **1** having an amino functional group at the meso position was prepared according to previous reports, and the structure of **1** is shown in Scheme 1. The preparation of **1** started from appropriate amounts of benzaldehyde and pyrrole giving TPP,[30] in which the *meso* position was then replaced by a nitro functional group according to the method of Adler *et al.*[25] The nitro group was reduced by means of the Béchamp manner[26] in the presence of $SnCl_2$ to yield the desired TPP derivative **1**. The amino group of **1** was allowed to react with acryl chloride **2** in the presence of an acid scavenger to produce the corresponding acrylamide **3** as crystals in 71% yield after chromatographic purification. Structural elucidation of the acrylamide **3** was done by a combination of spectroscopic analyses, MALDI-TOF MS, and elemental analysis, and the ^{1}H NMR spectrum of **3** in DMSO-d_6 is shown in Figure 2a. Aromatic ring protons, amine protons according to the pyrrole units, and acryl amide protons are clearly observed. In addition, two protons due to pyrrole's N−H were shielded to appear at −2.77 ppm because of the effect of the aromatic ring current in the porphyrin ring system.

A known glycomonomer **4** was prepared according to the method previously reported.[27] For the preparation of **4**, an oxazoline derivative[31] was condensed with 2-acrylamidoethan-1-ol in the presence of an acid catalyst[32] to afford the corresponding glycoside, which was further transformed by

https://doi.org/10.1021/acsomega.3c05581
ACS Omega 2023, 8, 37451−37460

Scheme 2. Polymer Synthetic Route of Glycopolymer 5[a]

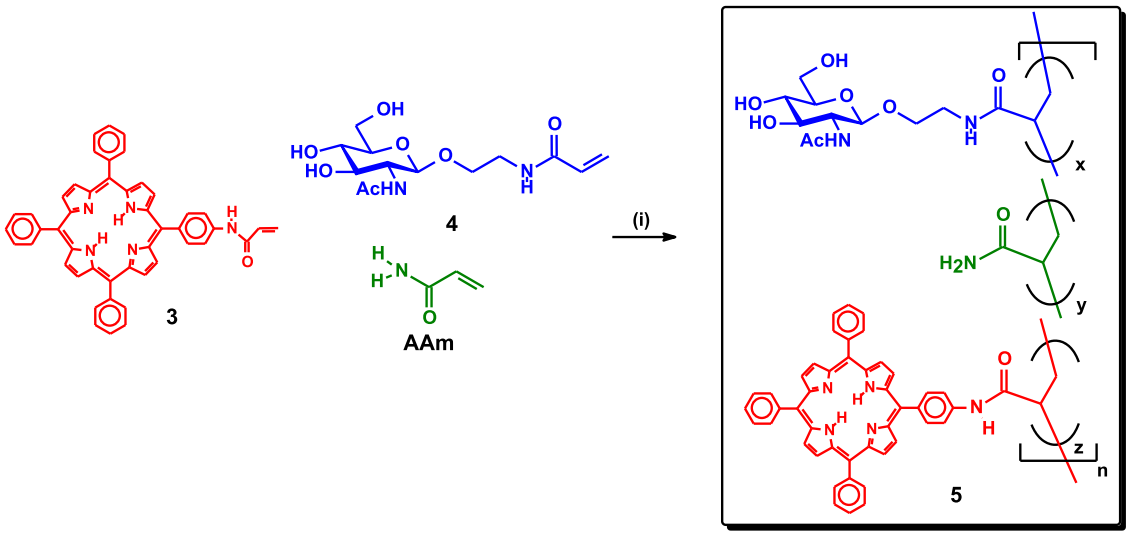

[a]Reagents and conditions: (i) azobis(isobutyronitrile) (AIBN), DMSO, rt, then 90 °C, 3 h, then 0.1 M AcOH−Pyr buffer (pH 5.00).

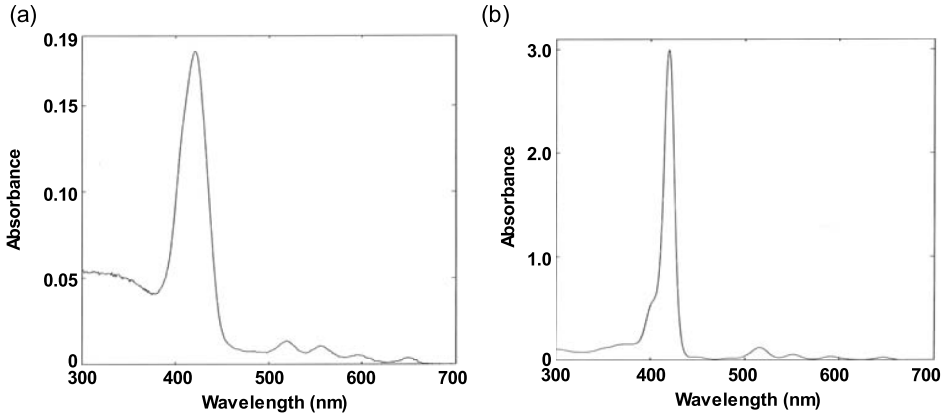

Figure 3. UV−vis spectra of 3.45 μM (based on TPP residual concentration) glycopolymer **5** having TPP moieties measured in H_2O at ambient temperature (a) and 8.22 μM TPP monomer **3** measured in $CHCl_3$ at ambient temperature (b).

means of Zemplén's trans esterification[33] to provide the desired glycomonomer **4**. A ^{1}H NMR spectrum of monomer **4** in D_2O is shown in Figure 2b.

Since the preparation of monomers **3** and **4** was efficiently accomplished, our attention was turned toward the polymer synthesis because of the preparation of a water-soluble porphyrin derivative. A schematic image is shown in Scheme 2. Thus, 0.1 molar equivalent of the TPP monomer **3**, glycosyl monomer **4**, and 10 molar equivalent of **AAm** were polymerized in DMSO in the presence of AIBN[34] to give brownish powdery glycopolymer **5** after lyophilization. The weight-average molecular weight ($\overline{Mw}$) of glycopolymer **5** was estimated to be 18,400 by means of size exclusion chromatography,[35] and structural elucidation was performed by ^{1}H NMR spectroscopic analysis as shown in Figure 2d. A ^{1}H NMR spectrum of the co-polymer prepared from GlcNAc monomer **4** and **AAm** without porphyrin moieties as a control glycopolymer[27] is shown in Figure 2c. In a comparison of the spectra in Figure 2c,d, aromatic ring protons of phenyl groups and amine protons attributed to the pyrrole units are clearly observed in the spectrum in Figure 2d, indicating incorporation of TPP moieties into the polymer backbone *via* covalent bonds. Previously, a similar polymer synthesis was carried out in an organic phase.[36−38] The polymer ratio of the glycopolymer **5** was estimated to be $x/y/z$ = 1:13:0.1 on the basis of the integral ratio of the anomeric proton of the GlcNAc/methine group of the polymer backbone at around 2.1 ppm and amine protons of pyrrole.

Characterization of the Water-Soluble Glycopolymer Having TPP Moieties. Given the preparation of a water-soluble glycopolymer **5** having TPP moieties as pendant top-like functionalities, our next objective was the investigation of the physical properties of **5** in comparison with those of the TPP derivative **3**. Figure 3 shows UV−vis spectra of both the TPP monomer **3** and glycopolymer **5** having TPP moieties. Since the glycopolymer **5** was dissolved in H_2O, UV−vis measurement was performed in an aqueous solution at ambient temperature. The results of the UV−vis measurement clearly indicated strong absorption at around 420 nm according to the Soret band and four weak absorptions at around 500 to 650 nm attributed to the Q band region that are characteristic absorptions of a porphyrin skeleton. The molar extinction coefficient of glycopolymer **5** was calculated to be 9.6×10^4 cm^{-1} M^{-1}. In addition, UV−vis spectroscopic analysis of TPP monomer **3** was carried out in $CHCl_3$ because of its insolubility in water, and a similar UV−vis profile for the

https://doi.org/10.1021/acsomega.3c05581
ACS Omega 2023, 8, 37451−37460

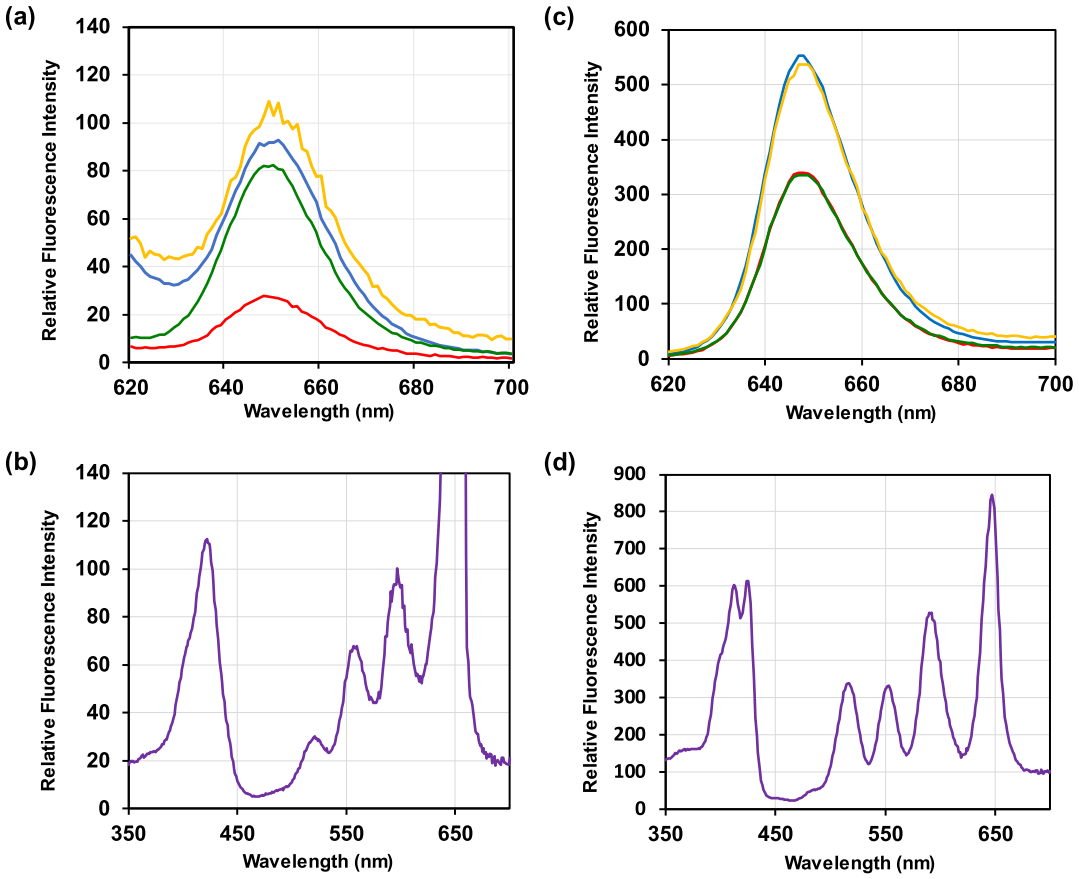

Figure 4. Emission spectra of 0.07 μM (based on TPP residual concentration) glycopolymer **5** having TPP moieties measured in H_2O at ambient temperature, yellow —: λ_{ex} 597 nm, green —: λ_{ex} 555 nm, red —: λ_{ex} 519 nm, and blue —: λ_{ex} 420 nm (a). Excitation spectrum of glycopolymer **5** having TPP moieties measured in H_2O at ambient temperature, λ_{em} 650 nm (b). Eemission spectra of 4.99 μM TPP monomer **3** measured in $CHCl_3$ at ambient temperature; yellow —: λ_{ex} 591 nm, green —: λ_{ex} 551 nm, red —: λ_{ex} 517 nm, and blue —: λ_{ex} 416 nm (c). Excitation spectrum of TPP monomer **3** measured in $CHCl_3$ at ambient temperature, λ_{em} 648 nm (d).

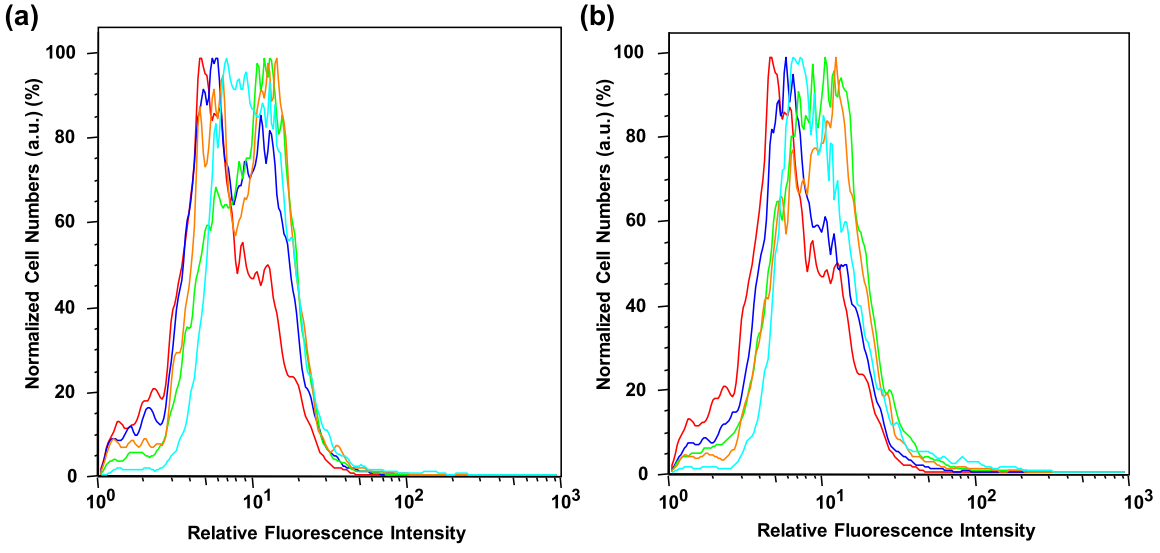

Figure 5. Flow cytometry measurement with excitation at λ_{ex} 440 nm detected at λ_{em} between 608−648 nm for various concentrations of glycopolymer **5** having TPP moieties with HeLa cells in PBS, pH 7.2−7.4, at ambient temperature; turquoise —: 7.5 μM, orange —: 2.5 μM green —: 1.0 μM blue —: 0.5 μM red —: 0 μM. (a) Intact. (b) In the presence of BioPOTER.

glycopolymer **5** was obtained. The molar extinction coefficient of monomer **3** was also calculated to be 3.6×10^5 cm^{-1} M^{-1}, and the value was 3.8 times higher than that of glycopolymer **5**. Although the differences could not be consistently compared because of the different solvent systems, the polymer showed moderate absorbance in aqueous media. The spectra indicated that the incorporation of TPP units into water-soluble

https://doi.org/10.1021/acsomega.3c05581
ACS Omega 2023, 8, 37451−37460

glycopolymer **5** was successfully accomplished by means of a simple radical polymerization method.

Since the unique profile of a water-soluble glycopolymer having TPP units was obtained, our next interest in the polymer was the ability of its fluorescence responses. Thus, the glycopolymer **5** was excited at various wavelengths corresponding to the Soret band and the Q band region in aqueous media, and the results showed fluorescence emissions at around 650 nm with each intensity [Figure 4a]. In order to confirm the origin of the emission at around the 650 nm, the excitation spectrum was investigated. The excitation spectrum is shown in Figure 4b and indicates a strong broad excitation peak at around 400 nm caused by the Soret band region and excitation peaks at around 500 to 650 nm caused by the Q band region, which is close to the profile for the UV−vis spectrum of the glycopolymer **5** as shown in Figure 3a. Further investigations were performed for the TPP monomer **3** as a fluorogenic standard molecule. The TPP monomer **3** was excited in the same manner as that described for glycopolymer **5** in $CHCl_3$ instead of H_2O, and similar emission spectra were obtained, as shown in Figure 4c. Strong emissions at around 650 nm were detected in each spectrum, and excitation spectra fixed emission at 650 nm, on the other hand, was recorded, as shown in Figure 4d. A spectrum similar to that shown in Figure 3b was obtained.

Biological Evaluations for the Water-Soluble Glycopolymer Having TPP Moieties by Means of Flow Cytometry for HeLa Cells. Biological evaluations of the glycopolymer **5** were further performed by means of flow cytometry for HeLa cells, which are frequently used as candidates of cancer cells.[29] HeLa cells were incubated with or without BioPOTER in the presence of various concentrations of the glycopolymer **5** in PBS at pH 7.2−7.4 for 4 h. After the usual workup, the HeLa cells were evaluated by using a flow cytometer at ambient temperature, and the results are shown in Figure 5. The fluorescence intensities of intact of Hela cells gradually increased according to the polymer concentration as shown in Figure 5a, and the relationship between the concentration of glycopolymer **5** and average fluorescence intensities are represented in Figure 6. In addition, the average fluorescence intensities are summarized in Table 1. The results suggested that the glycopolymer **5** having TPP units was incorporated into HeLa cells without any additional reagents. Since it is known that glycopolymers having an appropriate molecular weight are incorporated into cells by endocytosis,[39] the uptake of our polymer into HeLa cells might have occurred by a similar transportation system. In addition, DDS-associated reagents such as BioPOTER were used in the same incubation conditions as those described previously, and the results of flow cytometric analysis gave similar profiles as shown in Figure 5b, Table 1, and Figure 6. The results also supported incorporation of the glycopolymer **5** into HeLa cells. Uptake of glycopolymer **5** into HeLa cells was confirmed in the presence and absence of DDS-associated reagents.

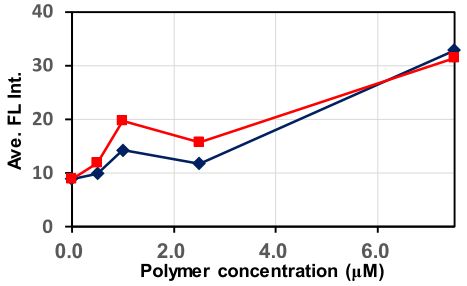

Figure 6. Relationship between the concentration of glycopolymer **5** having TPP moieties and average fluorescence intensities on the basis of flow cytometry measurement with excitation at λ_{ex} 440 nm detected at λ_{em} between 608−648 nm; red —: intact, dark blue —: in the presence of BioPOTER.

Table 1. Results of Flow Cytometric Analysis of Glycopolymer 5

	average fluorescence intensity	
polymer **5** (μM)	w/o	BioPOTER
7.5	32.9	31.5
2.5	11.8	15.7
1	14.3	19.7
0.5	9.92	11.9
0	8.93	8.93

Biological Evaluations of the Water-Soluble Glycopolymer Having TPP Moieties by Means of Microscopy for HeLa Cells. Because of confirmation of successful incorporation of the glycopolymer **5** into HeLa cells, direct investigation of HeLa cells in the presence of the glycopolymer **5** was further performed by microscopic analyses.[29] HeLa cells with no glycopolymer **5** as 0 μM were initially observed. Photos of the cells are shown in Figure 7a in the absence of serum and in Figure 7g in the presence of serum. From the results of cell observations according to Figure 7a−f, in the absence of serum in the medium, cell death occurred depending on the concentration of the glycopolymer **5**. It seems, therefore, that the decay of HeLa cells spontaneously occurred due to the cytotoxicity of the glycopolymer **5**. Treatment of HeLa cells with a cytotoxic ingredient was reported and showed apoptotic Hela cells' death.[40] A similar observation of the cells in the presence of serum was also made, and the results are shown in Figure 7g−l. The cytotoxicity of the glycopolymer **5** depending on the concentration of the glycopolymer was also investigated. In careful comparison with Figure 7f,l, the decay of HeLa cells was slightly avoided in the presence of serum as shown in Figure 7l. The results suggested that the cytotoxicity of the glycopolymer **5** was weaker in the presence of serum than in the absence of serum. The shape of HeLa cells was also examined by means of an apoptosis induction approach.[29] CHX, which is known as an apoptosis-inducing reagent, was added as control (in the absence of glycopolymer **5**) to the cell growth medium of HeLa cells both in the absence and presence of serum, and the results are shown in Figure 8. Although the dead cells in the presence of CTX showed a round-like shape in both Figure 8b,d, the dead cells in the presence of the glycopolymer **5** showed an ellipse-like shape[41] in Figure 7l. It was surprisingly found that cell death in the two conditions might be caused by different mechanisms.[42] The results suggest that the glycopolymer **5** showed cytotoxic activity for HeLa cells, which are cancer cells, and can be applied not only for PDT but also as an anti-cancer reagent.

CONCLUSIONS

In summary, we have shown the preparation of a glycopolymer having TPP moieties by means of simple radical polymerization of the corresponding glycomonomer, TPP monomer,

https://doi.org/10.1021/acsomega.3c05581
ACS Omega 2023, 8, 37451−37460

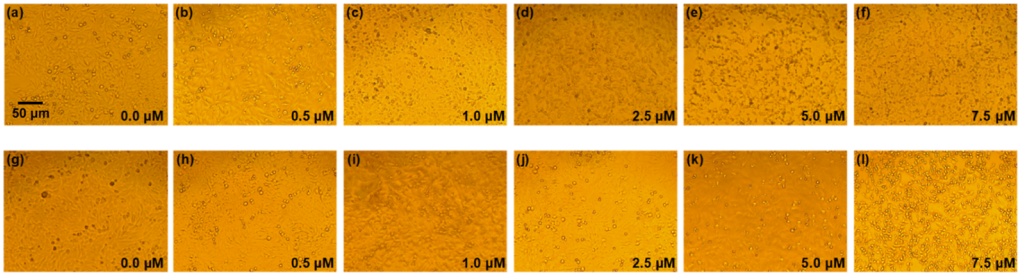

Figure 7. Observations of HeLa cells in the absence of serum (upper) and the presence of serum (lower). The concentrations are represented as added concentrations of glycopolymer **5** having TPP moieties; (a) 0.0, (b) 0.5, (c) 1.0, (d) 2.5, (e) 5.0, (f) 7.5 μM in the absence of serum, and (g) 0.0, (h) 0.5, (i) 1.0, (j) 2.5, (k) 5.0, (l) 7.5 μM in the presence of serum.

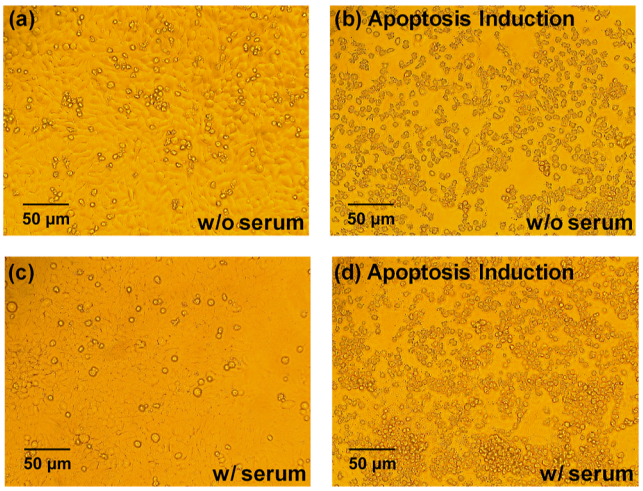

Figure 8. Observations of HeLa cells subjected to apoptosis induction treatment in the absence of serum (upper) and the presence of serum (lower). The left columns indicate HeLa cells without an apoptosis-inducing reagent. (a) No induction treatment in the absence of serum and (c) no induction treatment in the presence of serum. The right columns indicate HeLa cells with an apoptosis-inducing reagent. (b) Induction treatment in the absence of serum and (d) induction treatment in the presence of serum.

and **AAm**. Polymerization gave the desired water-soluble glycopolymers bearing TPP moieties as pendant top-like formats. It was noteworthy that synthetic assembly of a large amount of sugar moieties as highly hydrophilic portions and a small amount of TPP moieties as hydrophobic portions gave a unique water-soluble polymer, and the polymer showed remarkable biological activities for cancer cells. The findings indicate that polymer-support methodology is an effective approach for cancer cells. The combination of carbohydrate and TPP is very promising as an anti-cancer therapy. Further manipulations of the glycopolymers bearing TPP moieties are now underway, and the results will be reported elsewhere.

■ ASSOCIATED CONTENT

Supporting Information

The Supporting Information is available free of charge at https://pubs.acs.org/doi/10.1021/acsomega.3c05581.

^{1}H NMR and FT-IR spectra of the desired compound, GPC profile of the polymer, and full-scale cell observations in the absence and the presence of a serum (PDF)

■ AUTHOR INFORMATION

Corresponding Author

Koji Matsuoka − *Area for Molecular Function, Division of Material Science, Graduate School of Science and Engineering, Medical Innovation Research Unit (MiU), Advanced Institute of Innovative Technology (AIIT), and Health Sciences and Technology Research Area, Strategic Research Center, Saitama University, Sakura, Saitama 338-8570, Japan;* orcid.org/0000-0002-8987-2715; Phone: +81-70-8819-4601; Email: koji@fms.saitama-u.ac.jp

Authors

Yoshihiro Ishimaru − *Area for Molecular Function, Division of Material Science, Graduate School of Science and Engineering, Saitama University, Sakura, Saitama 338-8570, Japan*

Tomohide Moteki − *Area for Molecular Function, Division of Material Science, Graduate School of Science and Engineering, Saitama University, Sakura, Saitama 338-8570, Japan*

Miho Suzuki − *Area for Molecular Function, Division of Material Science, Graduate School of Science and Engineering, Saitama University, Sakura, Saitama 338-8570, Japan*

Tetsuo Koyama − *Area for Molecular Function, Division of Material Science, Graduate School of Science and Engineering, Saitama University, Sakura, Saitama 338-8570, Japan*

Takahiko Matsushita − *Area for Molecular Function, Division of Material Science, Graduate School of Science and Engineering, Medical Innovation Research Unit (MiU), Advanced Institute of Innovative Technology (AIIT), and Health Sciences and Technology Research Area, Strategic Research Center, Saitama University, Sakura, Saitama 338-8570, Japan*

Ken Hatano − *Area for Molecular Function, Division of Material Science, Graduate School of Science and Engineering, Medical Innovation Research Unit (MiU), Advanced Institute of Innovative Technology (AIIT), and Health Sciences and Technology Research Area, Strategic Research Center, Saitama University, Sakura, Saitama 338-8570, Japan*

Complete contact information is available at: https://pubs.acs.org/10.1021/acsomega.3c05581

Notes

The authors declare no competing financial interest.

https://doi.org/10.1021/acsomega.3c05581
ACS Omega 2023, 8, 37451−37460

REFERENCES

(1) Smith, K. M. *Porphyrins and Metalloporphyrins*; Elsevier Scientific Publishing Company, 1975.
(2) Hückel, E. Quantentheoretische Beiträge zum Benzolproblem. *Z. Phys.* **1931**, *70*, 204−286.
(3) Hückel, E. Quantentheoretische Beiträge zum Problem der Aromatischen und Ungesättigten Verbindungen. III. *Z. Phys.* **1932**, *76*, 628−648.
(4) Vogel, E. The Porphyrins From The Annulene Chemists Perspective. *Pure Appl. Chem.* **1993**, *65*, 143−152.
(5) Winkelman, J.; Slater, G.; Grossman, J. The Concentration in Tumor and Other Tissues of Parenterally Administered Tritium- and ^{14}C-labeled Tetraphenylporphinesulfonate. *Cancer Res.* **1967**, *27*, 2060−2064.
(6) Dailey, H. A.; Smith, A. Differential Interaction of Porphyrins Used In Photoradiation Therapy With Ferrochelatase. *Biochem. J.* **1984**, *223*, 441−445.
(7) Nishida, K.; Tojo, T.; Kondo, T.; Yuasa, M. Evaluation of the Correlation between Porphyrin Accumulation in Cancer Cells and Functional Positions for Application as a Drug Carrier. *Sci. Rep.* **2021**, *11*, 2046.
(8) Weishaupt, K. R.; Gomer, C. J.; Dougherty, T. J. Identification Of Singlet Oxygen As Cytotoxic Agent In Photo-Inactivation of A Murine Tumor. *Cancer Res.* **1976**, *36*, 2326−2329.
(9) Jocham, D.; Stepp, H.; Waidelich, R. Photodynamic Diagnosis in Urology: State-of-the-art. *Eur. Urol.* **2008**, *53*, 1138−1150.
(10) Josefsen, L. B.; Boyle, R. W. Unique Diagnostic and Therapeutic Roles of Porphyrins and Phthalocyanines in Photodynamic Therapy, Imaging and Theranostics. *Theranostics* **2012**, *2*, 916−966.
(11) Ethirajan, M.; Chen, Y.; Joshi, P.; Pandey, R. K. The Role of Porphyrin Chemistry in Tumor Imaging and Photodynamic Therapy. *Chem. Soc. Rev.* **2011**, *40*, 340−362.
(12) Abrahamse, H.; Hamblin, M. R. New Photosensitizers for Photodynamic Therapy. *Biochem. J.* **2016**, *473*, 347−364.
(13) Dolmans, D.; Fukumura, D.; Jain, R. K. Photodynamic Therapy for Cancer. *Nat. Rev. Cancer* **2003**, *3*, 380−387.
(14) Ntziachristos, V.; Bremer, C.; Weissleder, R. Fluorescence Imaging with Near-infrared Light: New Technological Advances that Enable *in vivo* Molecular Imaging. *Eur. Radiol.* **2003**, *13*, 195−208.
(15) Huang, Z. A Review of Progress in Clinical Photodynamic Therapy. *Technol. Cancer Res. Treat.* **2005**, *4*, 283−293.
(16) Yano, S.; Hirohara, S.; Obata, M.; Hagiya, Y.; Ogura, S.; Ikeda, A.; Kataoka, H.; Tanaka, M.; Joh, T. Current States and Future Views in Photodynamic Therapy. *J. Photochem. Photobiol. C* **2011**, *12*, 46−67.
(17) Weaver, J. A.; Hambright, P. Kinetics of the Incorporation of Copper(II) into a Water-soluble Porphyrin. *Inorg. Chem.* **1969**, *8*, 167−168.
(18) Stein, T. P.; Plane, R. A. Incorporation of Zinc Ion into a Synthetic Water-soluble Porphyrin. *J. Am. Chem. Soc.* **1969**, *91*, 607−610.
(19) Itoh, J. I.; Yotsuyanagi, T.; Aomura, K. Spectrophotometric Determination of Copper with α, β, γ, δ-Tetraphenylporphine Trisulfonate. *Anal. Chim. Acta* **1975**, *74*, 53−60.
(20) Maillard, P.; Gaspard, S.; Guerquin-Kern, J. L.; Momenteau, M. Glycoconjugated Tetrapyrrolic Macrocycles. *J. Am. Chem. Soc.* **1989**, *111*, 9125−9127.
(21) Momenteau, M.; Maillard, P.; De Bélinay, M. A.; Carrez, D.; Croisy, A. Tetrapyrrolic Glycosylated Macrocycles for an Application in PDT. *J. Biomed. Opt.* **1999**, *4*, 298−318.
(22) Sol, V.; Chaleix, V.; Champavier, Y.; Granet, R.; Huang, Y. M.; Krausz, P. Glycosyl Bis-porphyrin Conjugates: Synthesis and Potential Application in PDT. *Bioorg. Med. Chem.* **2006**, *14*, 7745−7760.
(23) Matsuoka, K.; Nakagawa, M.; Koyama, T.; Matsushita, T.; Hatano, K. Systematic Synthesis of a Series of Glycopolymers having *N*-Acetyl-D-glucosamine Moieties that Can Be Used for Evaluations of Lectin-Carbohydrate Interactions. *Eur. Polym. J.* **2022**, *168*, 111101.
(24) Luguya, R.; Jaquinod, L.; Fronczek, F. R.; Vicente, M. H.; Smith, K. M. Synthesis and Reactions of *meso*-(*p*-Nitrophenyl)-porphyrins. *Tetrahedron* **2004**, *60*, 2757−2763.
(25) Adler, A. D.; Longo, F. R.; Finarelli, J. D.; Goldmacher, J.; Assour, J.; Korsakoff, L. A Simplified Synthesis for *meso*-Tetraphenylporphine. *J. Org. Chem.* **1967**, *32*, 476.
(26) Béchamp, A. De L'action des Protosels de fer sur la Nitronaphtaline et la Nitrobenzine. Nouvelle Méthode de Formation des bases Organiques Artificielles de Zinin. *Ann. Chim. Phys.* **1854**, *42*, 186−196.
(27) Matsuoka, K.; Yamashita, S.; Koyama, T.; Matsushita, T.; Hatano, K. Verification of Suitable Ratio of Carbohydrate Residues in a Glycopolymer having GlcNAc Moieties for Determining the Affinity for Wheat Germ Agglutinin. *J. Mol. Struct.* **2020**, *1217*, 128404.
(28) Matsuoka, K.; Goshu, Y.; Takezawa, Y.; Mori, T.; Sakamoto, J. I.; Yamada, A.; Onaga, T.; Koyama, T.; Hatano, K.; Snyder, P. W.; et al. Practical Synthesis of Fully Protected Globotriaose and Its Glycopolymers. *Carbohydr. Polym.* **2007**, *69*, 326−335.
(29) Suzuki, M.; Sakata, I.; Sakai, T.; Tomioka, H.; Nishigaki, K.; Tramier, M.; Coppey-Moisan, M. A High-throughput Direct Fluorescence Resonance Energy Transfer-based Assay for Analyzing Apoptotic Proteases using Flow Cytometry and Fluorescence Lifetime Measurements. *Anal. Biochem.* **2015**, *491*, 10−17.
(30) Rothemund, P. Formation of Porphyrins from Pyrrole and Aldehydes. *J. Am. Chem. Soc.* **1935**, *57*, 2010−2011.
(31) Nakabayashi, S.; Warren, C. D.; Jeanloz, R. W. A New Procedure For The Preparation of Oligosaccharide Oxazolines. *Carbohydr. Res.* **1986**, *150*, C7−C10.
(32) Nishimura, S.; Matsuoka, K.; Kurita, K. Synthetic Glycoconjugates - Simple and Potential Glycoprotein Models Containing Pendant *N*-Acetyl-D-Glucosamine And *N,N′*-Diacetylchitobiose. *Macromolecules* **1990**, *23*, 4182−4184.
(33) Zemplén, G.; Pacsu, E. Über die Verseifung Acetylierter Zucker und Verwandter Substanzen. *Ber. Dtsch. Chem. Ges.* **1929**, *62*, 1613−1614.
(34) Matsuoka, K.; Takita, C.; Koyama, T.; Miyamoto, D.; Yingsakmongkon, S.; Hidari, K.; Jampangern, W.; Suzuki, T.; Suzuki, Y.; Hatano, K.; et al. Novel Linear Polymers Bearing Thiosialosides as Pendant-type Epitopes for Influenza Neuraminidase Inhibitors. *Bioorg. Med. Chem. Lett.* **2007**, *17*, 3826−3830.
(35) Adachi, R.; Matsushita, T.; Koyama, T.; Hatano, K.; Matsuoka, K. Synthetic Assembly of a Series of Glycopolymers having Sialyl α 2-3 Lactose Moieties Connected with Longer Spacer Arms. *Bioorg. Med. Chem.* **2023**, *81*, 117209.
(36) Hasegawa, E.; Nemoto, J. I.; Kanayama, T.; Tsuchida, E. Syntheses and Properties of Vinyl Monomers Containing a *meso*-Tetraphenylporphin Ring and Their Copolymers. *Eur. Polym. J.* **1978**, *14*, 123−127.
(37) Kajiwara, A.; Aramata, K.; Nomura, S.; Morishima, Y.; Kamachi, M. Radical Polymerization of 5-(4-Acrylamido)-Phenyl-10,15,20-Triphenylporphyrin. *Chem. Lett.* **1992**, *21*, 95−98.
(38) Tay, T.; Turk, H.; Say, R. Synthesis of 5-(4-Methacrylamidophenyl)-10,15,20-triphenylporphyrin, its Copolymerization with Acrylamide and EDMA, Use of this Copolymer in the Adsorption of Bovine Serum Albumin. *React. Funct. Polym.* **2007**, *67*, 999−1007.
(39) Uemura, S.; Feng, F.; Kume, M.; Yamada, K.; Kabayama, K.; Nishimura, S. I.; Igarashi, Y.; Inokuchi, J. I. Cell Growth Arrest by Sialic Acid Clusters in Ganglioside GM3 Mimetic Polymers. *Glycobiology* **2007**, *17*, 568−577.
(40) Nurkhasanah; Azimahtol Hawariah Lope, P.; Jalifah, L. Morphological Studies of Apoptotic HeLa Cells Death Induced by Eurycomanone. *Indones. J. Pharm.* **2009**, *20*, 190−197.
(41) Rello, S.; Stockert, J. C.; Moreno, V.; Gamez, A.; Pacheco, M.; Juarranz, A.; Canete, M.; Villanueva, A. Morphological Criteria to Distinguish Cell Death Induced by Apoptotic and Necrotic Treatments. *Apoptosis* **2005**, *10*, 201−208.
(42) Miller, M. L.; Andringa, A.; Elliott, J.; Conwell Ii, K.; Dixon, K.; Carty, M. P. The Morphological and Spectral Phenotype of Apoptosis

https://doi.org/10.1021/acsomega.3c05581
ACS Omega 2023, 8, 37451−37460

in HeLa Cells Varies Following Exposure to UV-C and the Addition of Inhibitors of ICE and CPP32. *Cell Proliferation* **1998**, *31*, 17−33.

https://doi.org/10.1021/acsomega.3c05581
ACS Omega 2023, 8, 37451−37460